

Supporting Information

An Aggregation-Induced Emission (AIE) Active Probe Renders Al(III) Sensing and Tracking of Subsequent Interaction with DNA

Soham Samanta,^a Sudeep Goswami,^b Md. Najbul Hoque,^a Aiyagari Ramesh,^b and Gopal Das*,^a*

^a Department of Chemistry

Indian Institute of Technology Guwahati, Guwahati 781039, Assam, India

E-mail: gdas@iitg.ernet.in (Gopal Das)

^b Department of Biotechnology

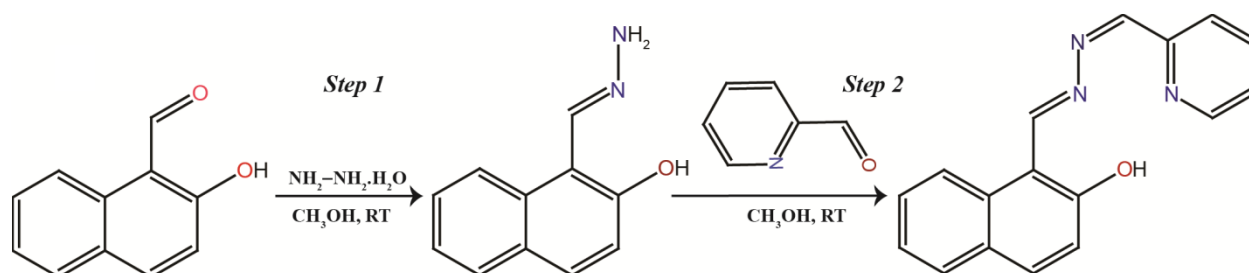
Indian Institute of Technology Guwahati, Guwahati 781039, Assam, India

E-mail: aramesh@iitg.ernet.in (Aiyagari Ramesh)

EXPERIMENTAL SECTION

General Information and Materials. All the materials for synthesis were purchased from commercial suppliers and used without further purification. The absorption spectra were recorded on a Perkin-Elmer Lambda-25 UV-vis spectrophotometer using 10 mm path length quartz cuvettes in the range of 250–800 nm wavelength, while fluorescence measurements were performed on a Horiba Fluoromax-4 spectrofluorometer using 10 mm path length quartz cuvettes with a slit width of 3 nm at 298 K. The mass spectrum of the ligand **L** was obtained using Waters Q-ToF Premier mass spectrometer. NMR spectra were recorded on a BRUKER Ascend-600 MHz instrument. The chemical shifts were recorded in parts per million (ppm) on the scale. The following abbreviations are used to describe spin multiplicities in ^1H NMR spectra: s = singlet; d = doublet; t = triplet; m = multiplet.

Synthesis of the probe L. In a 100ml round bottomed flask 10mmol (1.72g) of 2-hydroxy-1-naphthaldehyde was taken and it was dissolved in 50 mL of methanol by constant stirring. To this solution, excess of hydrazine hydrate (5.0 mL, ~100 mmol) was added. The mixture was allowed to stir for 24 h to obtain pale yellow colour solid product which was filtered and washed thoroughly with methanol. This product constituted the Schiff base having mono-imine bond and a free amine group of hydrazine (See scheme S1, step1, ESI).



Scheme S1: Synthesis of the probe **L**

In the next step 1.0 mmol of this product of obtained in step1 was dissolved in methanol and 1.1 mmol of 2-pyridinecarboxaldehyde was added and the mixture was stirred for 18 h to obtain a deep yellow colored solid product (See scheme S1, step 2, ESI) which was washed several times with methanol and then dried in a desiccator.

Crystallization of L. A small quantity of yellow powder of **L** (0.027 mM) was taken in a test tube containing DCM and stirred for few minutes to obtain a clear solution. Then solution was allowed to evaporate slowly and after one week X-ray mountable needle shaped yellow colored crystals appeared at the bottom of test tube.

Calculated yield: 81%. ^1H NMR [600 MHz, CDCl_3 , TMS, J (Hz), δ (ppm)]: 13.28 (1H, s), 9.80 (1H, s), 8.75 (1H, s), 8.17 (1H, d, $J=8.4$), 8.09 (1H, d, $J=7.8$), 7.90-7.79 (3H, m), 7.58 (1H, t, $J=7.8$), 7.43-7.37 (2H, m), 7.27-7.23 (2H, m), 7.26 (1H, s, CDCl_3). ^{13}C NMR [100 MHz, CDCl_3 , TMS, δ (ppm)]: 163.42, 161.87, 161.64, 150.45, 136.87, 135.36, 133.10, 129.44, 128.39, 128.26, 125.37, 124.00, 122.99, 120.23, 119.48, 119.37, 108.35. ESI-MS (positive mode, m/z)
Calculated for $\text{C}_{17}\text{H}_{13}\text{N}_3\text{O}$: 276.11. Found: 276.1315 [$(\text{M}+\text{H}^+)$].

Crystallographic Refinement Details. The crystallographic data and details of data collection of **L** is given in Table S2. In each case, a crystal of suitable size was selected from the mother liquor and immersed into silicone oil, then mounted on the tip of a glass fiber and cemented using epoxy resin. Intensity data for the all crystals were collected Mo-K α radiation ($\lambda = 0.71073\text{\AA}$) at 298(2) K, with increasing ω (width of 0.3° per frame) at a scan speed of 6 s/ frame on a Bruker SMART APEX diffractometer equipped with CCD area detector. The data integration and reduction were processed with SAINT¹ software. An empirical absorption correction was applied to the collected reflections with SADABS.² The structures were solved by direct methods using SHELXTL³ and were refined on F^2 by the full-matrix least-squares technique using the SHELXL-97 program package.⁴ Graphics are generated using MERCURY 3.0.⁵ In all cases, non-hydrogen atoms are treated anisotropically. The hydrogen atoms are located on a difference Fourier map and refined. In other cases, the hydrogen atoms are geometrically fixed.

UV–Vis and fluorescence spectroscopic studies. Stock solutions of various ions (1×10^{-3} mol L⁻¹) were prepared in deionized water. A stock solution of **L** (5×10^{-3} mol L⁻¹) was prepared in DMSO. The solution of **L** was then diluted to 10×10^{-6} mol L⁻¹ with CH₃OH/aqueous HEPES buffer (5mM, pH 7.3; 9:1, v/v). In titration experiments, a quartz optical cell of 1 cm path length was filled with a 2.0 mL solution of **L** to which the ion stock solutions were gradually added using a micropipette. In selectivity experiments, the test samples were prepared by placing appropriate amounts of the cations stock into 2.0 mL of **L** solution (10×10^{-6} mol L⁻¹). For fluorescence measurements, excitation was provided at 400 nm, and emission was acquired from 420 nm to 700 nm.

Detection Limit. The detection limits were calculated on the basis of the fluorescence titration (for Al^{3+}) and UV-Vis titration (for Cu^{2+}). The fluorescence emission spectrum or UV-Vis spectrum of **L** was measured 10 times, and the standard deviation of blank measurement was achieved. To gain the slope, the fluorescence emission at 537 nm was plotted as a concentration of Al^{3+} and absorbance at 502 nm was plotted as a concentration of Cu^{2+} . The detection limits were calculated using the following equation:

$$\text{Detection limit} = 3\sigma/k \quad (1)$$

where σ is the standard deviation of blank measurement, and k is the slope between the fluorescence emission intensity versus $[\text{Al}^{3+}]$ or absorbance versus $[\text{Cu}^{2+}]$.

Dynamic light scattering studies. The particle size of the **L**- Al^{3+} aggregates was measured by dynamic light scattering (DLS) experiments on a Malvern Zetasizer Nano ZS instrument equipped with a 4.0 mW He-Ne laser operating at a wavelength of 633 nm. The samples and the background were measured at room temperature (25°C) at a scattering angle of 173°. DLS experiments were carried out with an optically clear solution of **L** (10 μM) in MeOH in the presence of 1 equivalent and 10 equivalents of Al^{3+} ion. The solution was equilibrated for 30 minutes before taking the measurements.

Atomic Force Microscope (AFM) Studies. The overall morphology of the **L** was investigated from NT-MDT micro-40 AFM instrument using a semicontact mode at a scan rate of 1 Hz. To a solution of **L** (10 μM) in mixed aqueous-organic ($\text{H}_2\text{O}/\text{MeOH}$, 1:9, v/v) medium 10 equivalents of Al^{3+} was added and mixed well then it was drop-casted on a cover slip and left open to atmosphere for 12 h, followed by dessication prior to acquiring AFM images.

Field Emission Scanning Electron Microscope (FESEM) Studies. The morphology of L-Al³⁺ complex was ascertained in a Jeol JEM 6700 field emission scanning electron microscope (FESEM). To a solution of L (10 µM) in mixed aqueous-organic (H₂O/MeOH, 1:9, v/v) medium 10 equivalents of Al³⁺ was added and mixed well then it was drop-casted on cover slip and left open to atmosphere for 12 h, followed by dessication prior to acquiring FESEM images.

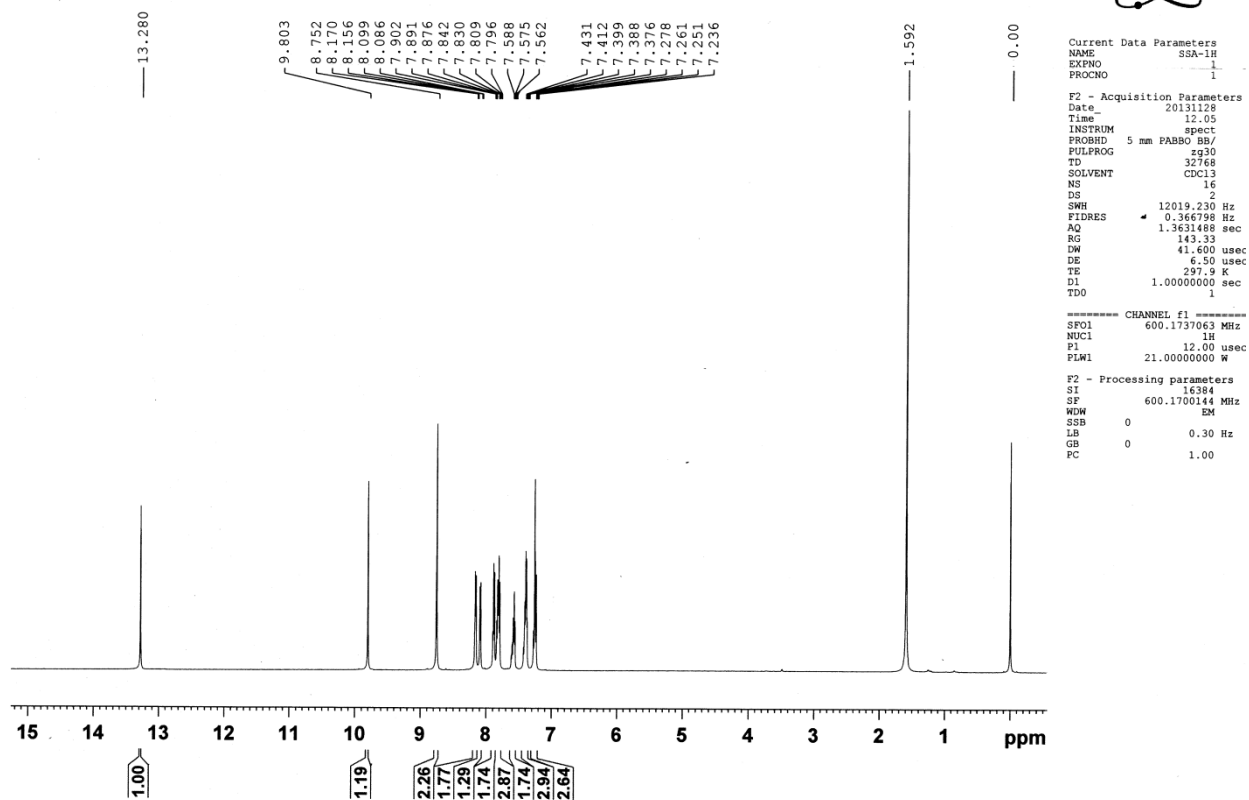
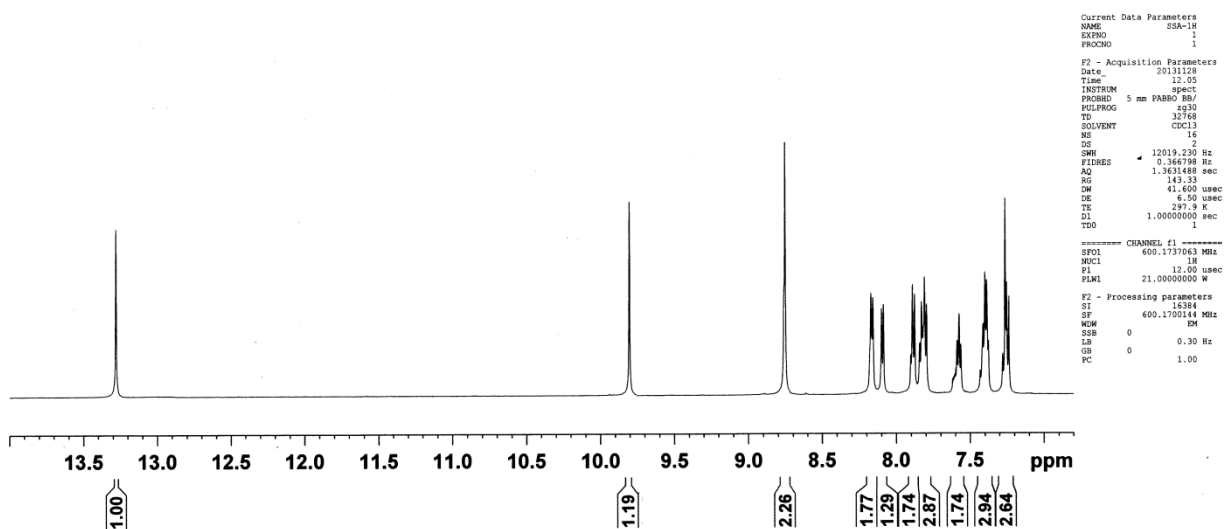
Cytotoxic Effect on HeLa Cells. The cytotoxic effect of the ligand and ligand-aluminium complex on cultured HeLa cells was determined by an MTT assay as per the manufacturer instruction (Sigma-Aldrich, MO, USA). HeLa cells were initially grown in a 25 cm² tissue culture flask in DMEM medium supplemented with 10% (v/v) FBS, penicillin (100 µg/mL) and streptomycin (100 µg/mL) under a humidified atmosphere of 5% CO₂ in an incubator until the cells were approximately 90% confluent. Prior to MTT assay, cells were trypsinized and seeded into 96-well tissue culture plates at a cell-density of 10⁴ cells per well and incubated with varying concentrations (12, 24, 36, 48, 60, 72, 84 and 96 µM) of the ligand, ligand-aluminium complex and the metal salt solution made in methanol solvent (0.1% v/v) and incubated for a period of 24 h under 5% CO₂. Solvent control samples (cells incubated in 0.1% methanol) were also included in parallel sets. Following incubation, the growth media was carefully aspirated, and fresh DMEM containing MTT solution was added to the wells. The plate was incubated for 4 h at 37°C. Following incubation, the supernatant was collected and the insoluble colored formazan product was solubilized in DMSO and its absorbance was measured in a microtiter plate reader (Infinite M200, TECAN, Switzerland) at 550 nm. The assay was performed in six sets for each concentration of the test samples. Data analysis and determination of standard deviation was performed with Microsoft Excel 2010 (Microsoft Corporation). In the MTT assay, the absorbance for the solvent control cells was considered as 100% cell viability and the absorbance

for the treated cells was compared to determine % cell viability with respect to the solvent control.

Cell Imaging Studies. HeLa cells were initially cultured in a 25 cm² tissue culture flask as mentioned before. Cells were then seeded into a 6 well plate and grown till 80% confluency in a CO₂ incubator at 37°C. The cells were washed thrice with sterile phosphate buffered saline (PBS) and incubated with 5.0 µM **L** in DMEM at 37°C for 1 h in a CO₂ incubator. The cells were again washed thrice with sterile PBS to remove the free ligand and bright field and dark field images were acquired using an epifluorescence microscope (Nikon eclipse Ti) having a filter that allowed blue light excitation at 445-495 nm. Subsequently, the cells were incubated in sterile PBS with 50 µM of aluminium chloride salt for 1 h and washed thoroughly with sterile PBS. Bright field and dark field images of the cells were again acquired in an epifluorescence microscope as mentioned before.

Interaction of L-Al³⁺ Ensemble with Calf Thymus DNA. In this experiment formation of L-Al³⁺ ensemble was initially accomplished by mixing 1.0 equivalent of the ligand with 10 equivalent of Al³⁺ solution as mentioned before. Subsequently the emission spectra were recorded by varying the concentrations of calf thymus DNA (30 µM-330 µM) which was added in appropriate amount using micropipette to the L-Al³⁺ ensemble. The fluorescence emission spectra of the samples were recorded in a spectrofluorometer in a scanning mode from 420 nm to 700 nm by setting the excitation wavelength at 400 nm.

SSA-1H

Figure S1. ^1H -NMR spectra of **L**.Figure S2. Expanded ^1H -NMR spectra of **L**.

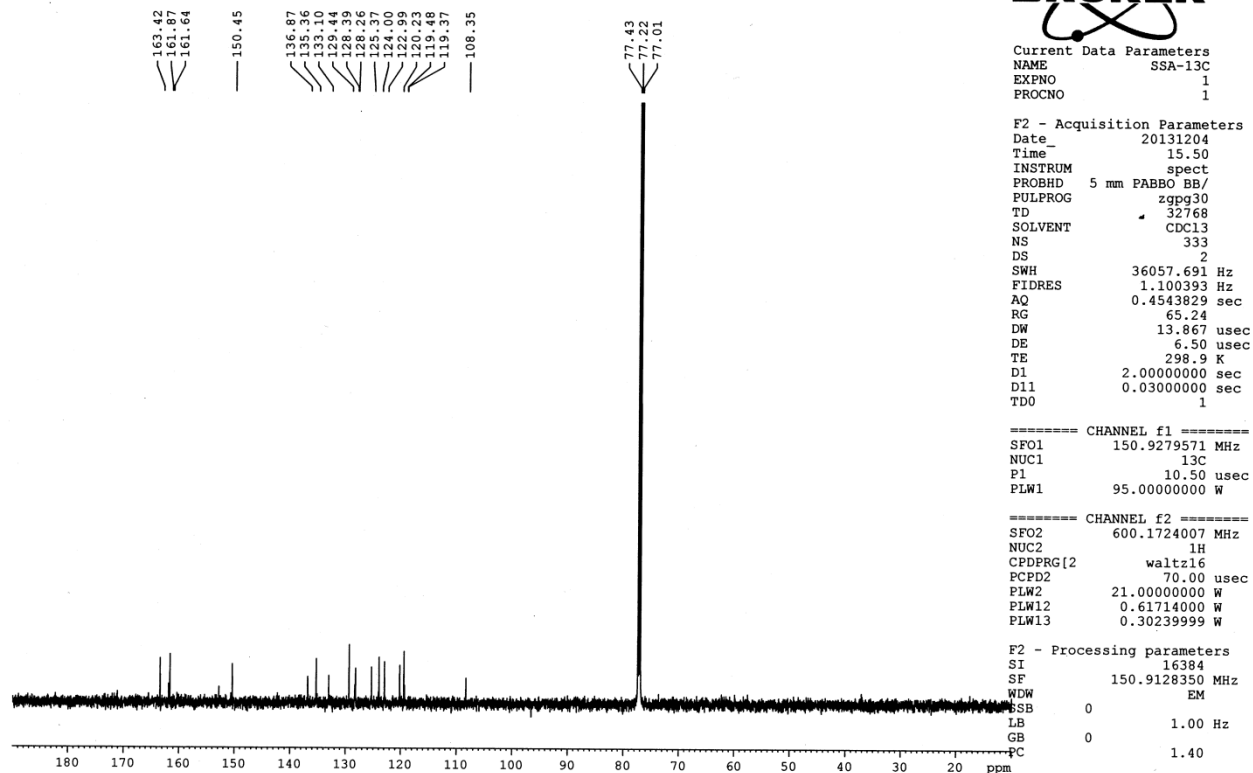
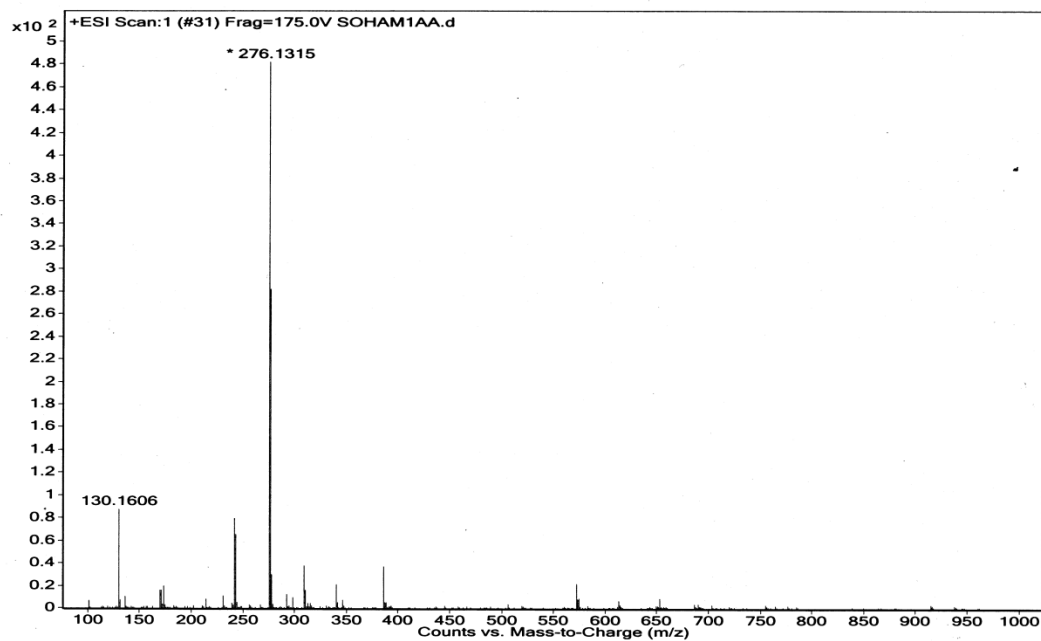
Figure S3. ^{13}C -NMR spectra of L.

Figure S4. Mass spectrum of L.

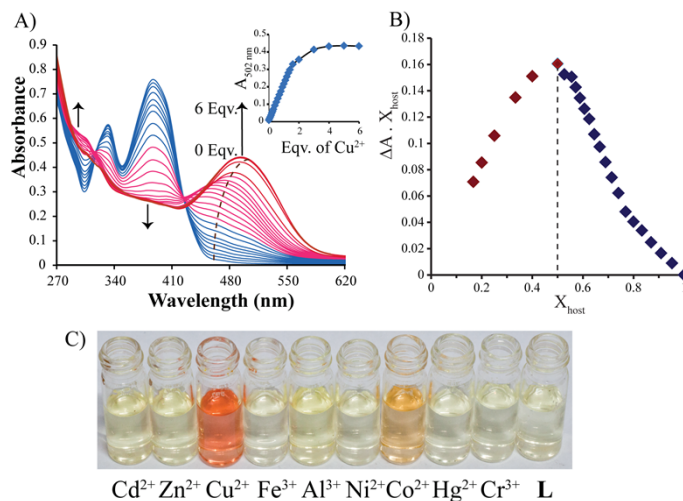


Figure S5. (A) UV-vis spectra of L (10 μM) in presence of varying concentration of Cu²⁺. INSET: Changes in the absorbance at 502 nm with concentration of Cu²⁺ (B) Job's plot for L-Cu²⁺ complex formation using UV-visible titration experiment. (C) Visual color change of L in presence of different metal ions in daylight.

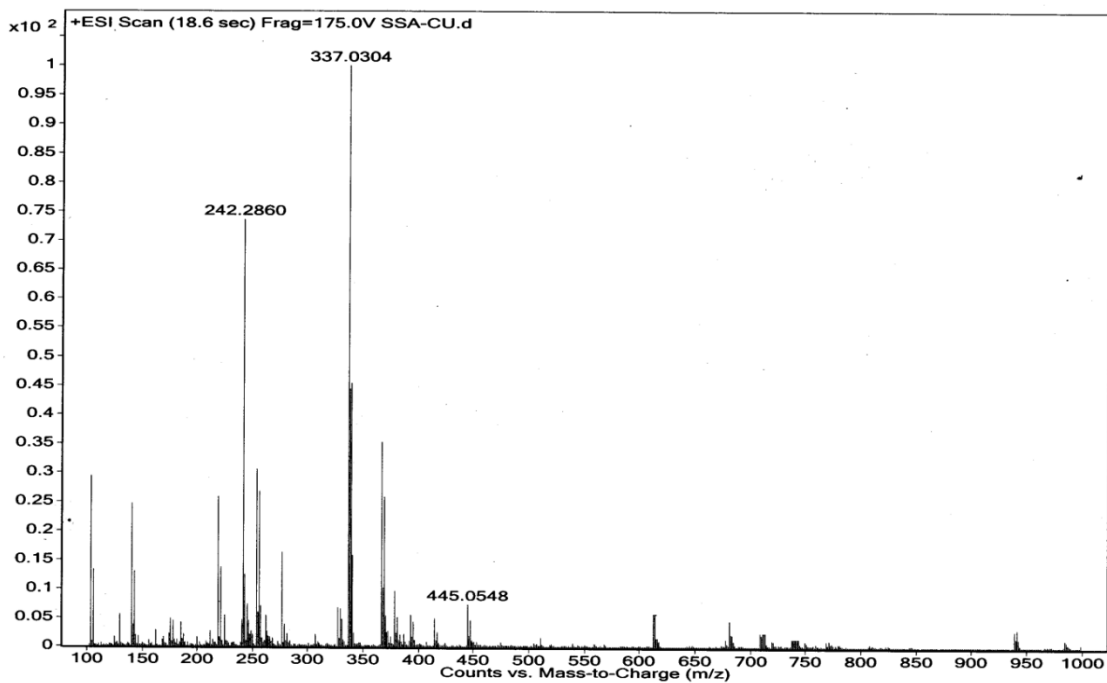


Figure S6. Mass spectrum of L-Cu²⁺ complex.

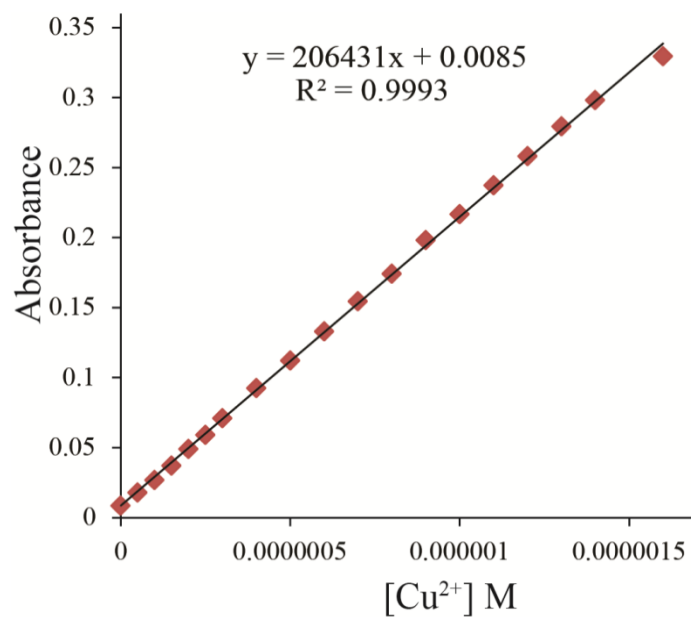


Figure S7. Absorbance versus concentration plot for measuring the detection limit ($3\sigma/k$, $\sigma = 0.0000753$) of Cu^{2+} by **L**.

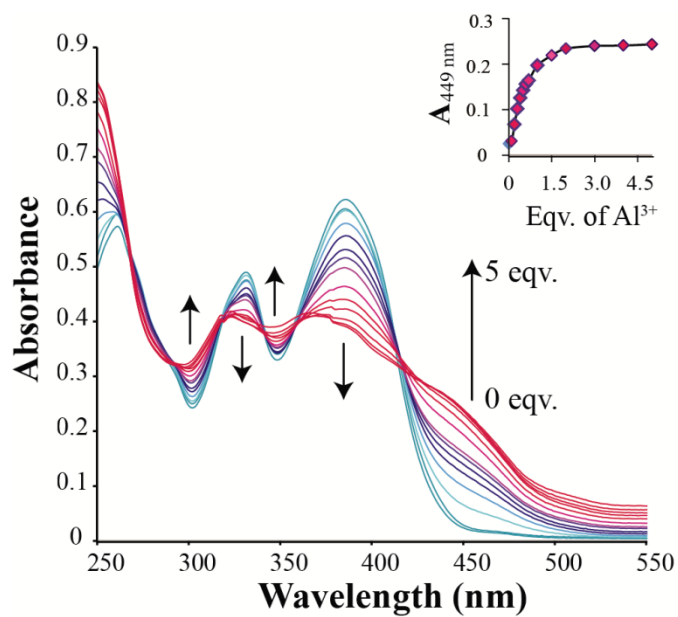


Figure S8. UV-visible titration experiment of **L** with Al^{3+} .

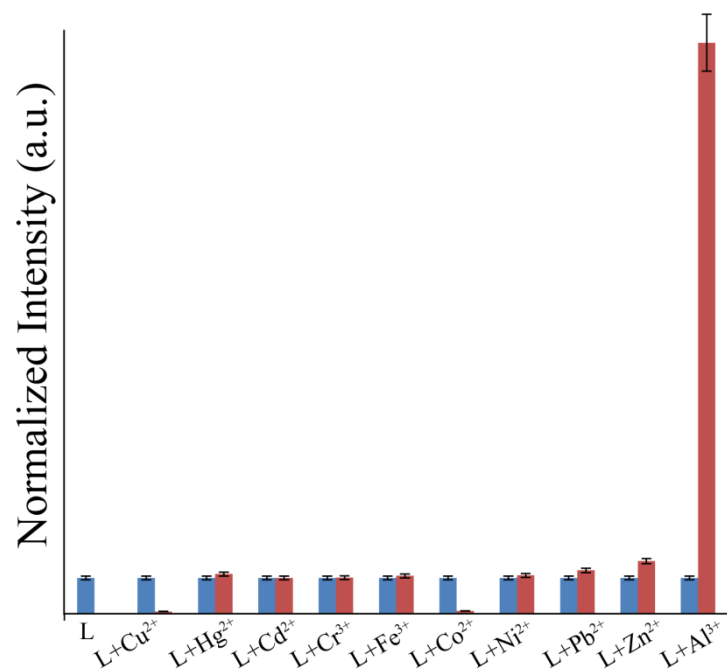


Figure S9. Comparison of fluorescence intensity of **L** on interaction with various metal ions.

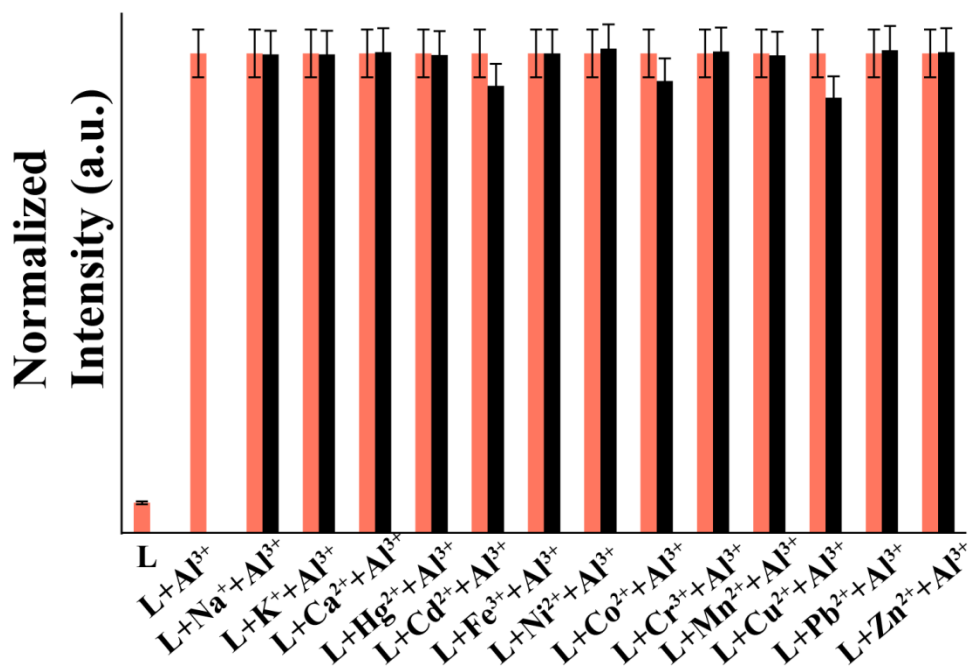


Figure S10. Effect of various metal ions on the fluorescence intensity of **L+Al³⁺**.

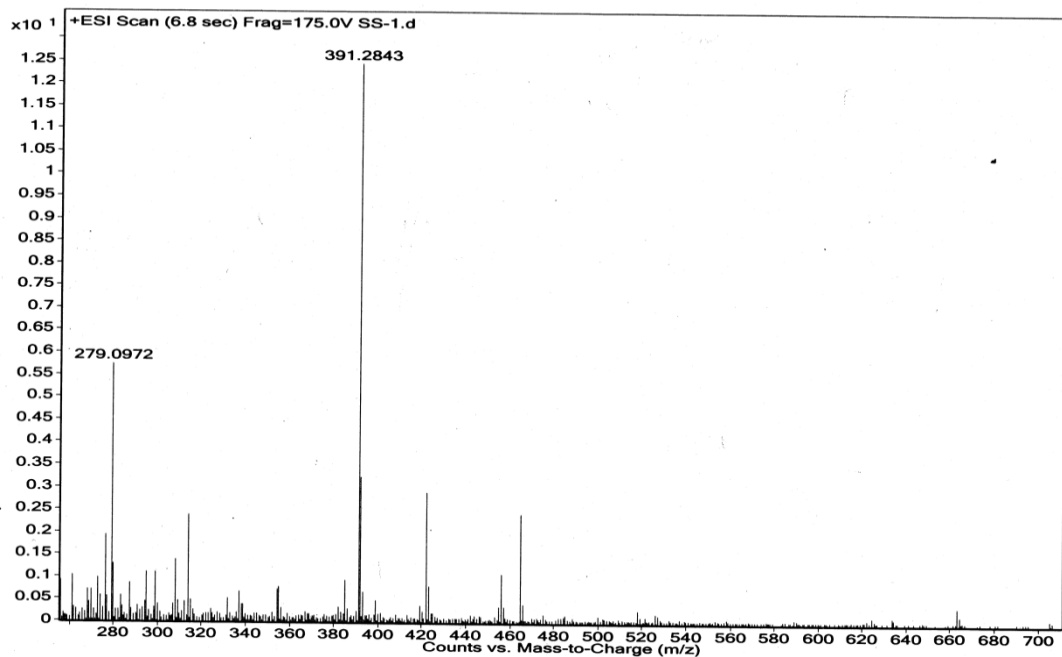


Figure S11. Mass spectrum of L-Al³⁺ complex.

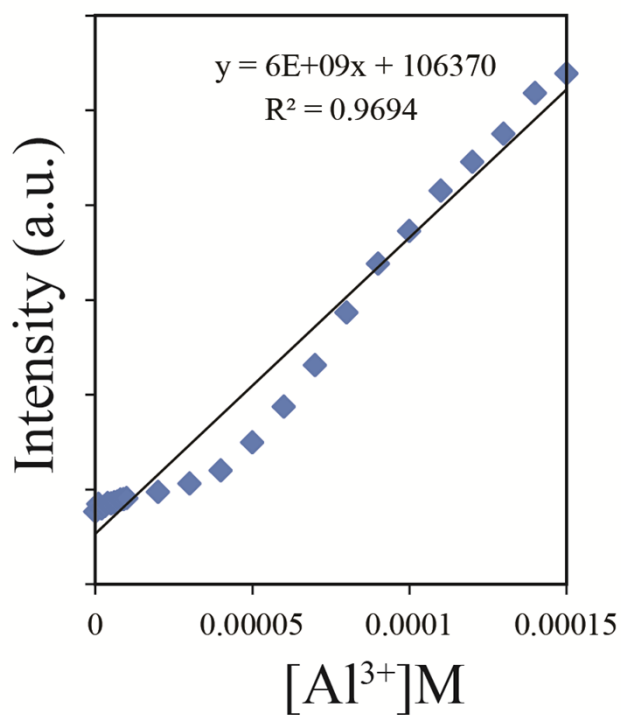


Figure S12. Determination of detection limit of L (10 μ M) for Al³⁺ by fluorescence titration experiment.

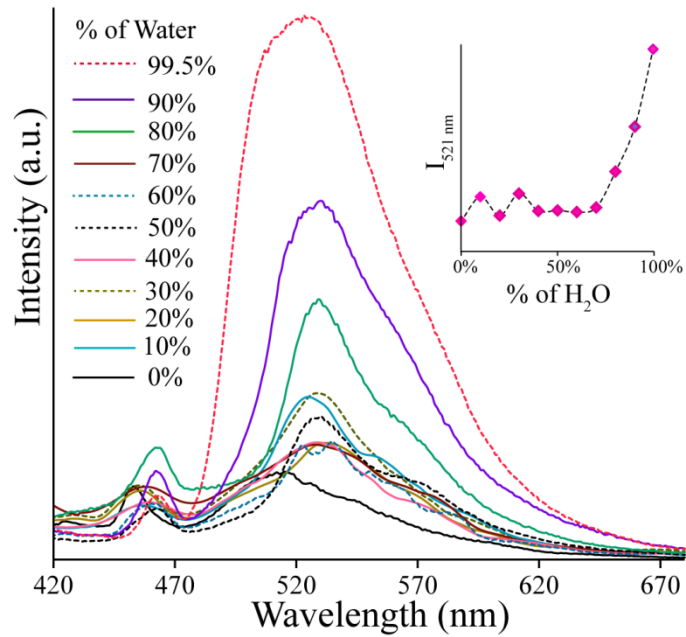


Figure S13. Fluorescence emission spectra of **L** (10 μ M) in different ratios of H₂O/MeOH at λ_{ex} = 400 nm.

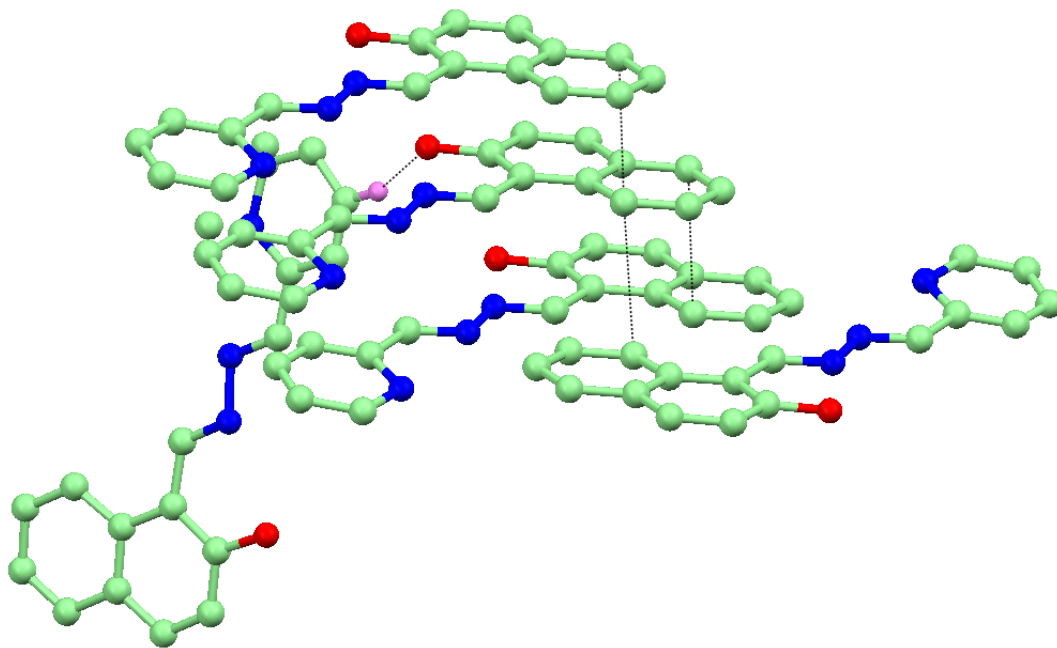


Figure S14. C–H \cdots O and $\pi\cdots\pi$ interaction in the probe **L**.

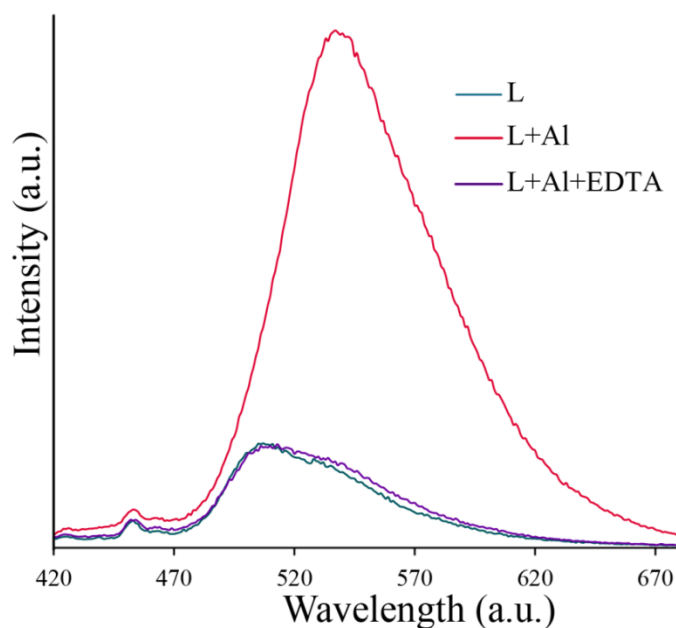


Figure S15. Fluorescence spectra of **L** (10 μM) in presence of 10 equivalents of Al^{3+} before and after treatment with excess EDTA. $\lambda_{\text{ex}} = 400 \text{ nm}$.

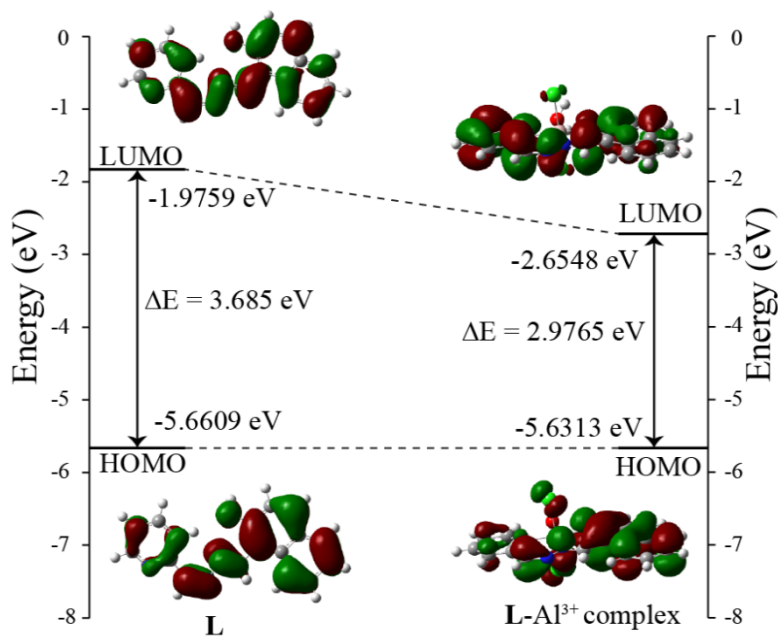


Figure S16. Frontier molecular orbital plots and energy level diagrams of **L** and **L-Al³⁺** complex. The calculations were performed using B3LYP/6-31 G (d,p) as implemented on Gaussian 03.

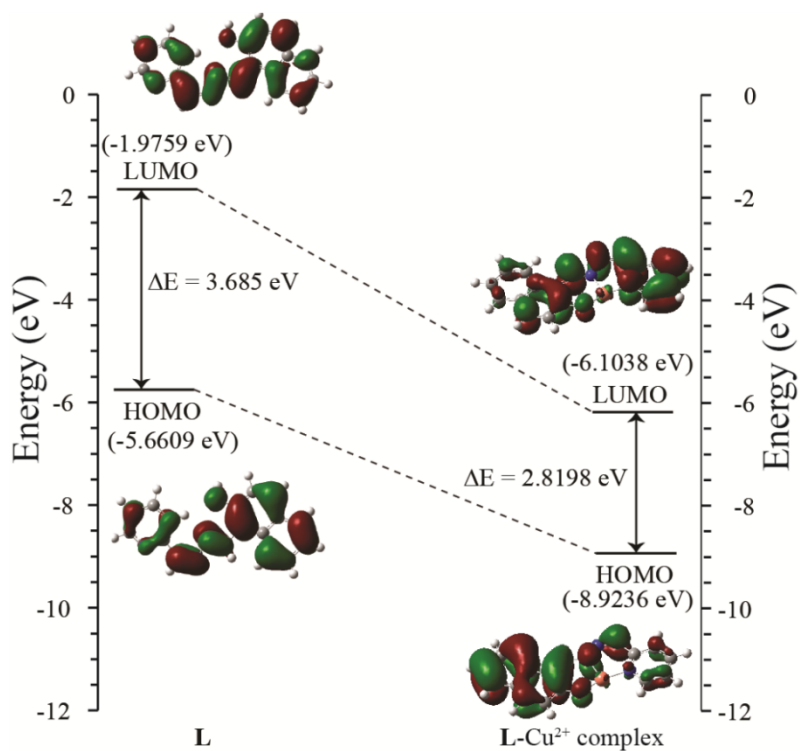


Figure S17. Frontier molecular orbital plots and energy level diagrams of **L** and **L-Cu²⁺** complex. The calculations were performed using B3LYP/6-31 G (d,p) as implemented on Gaussian 03.

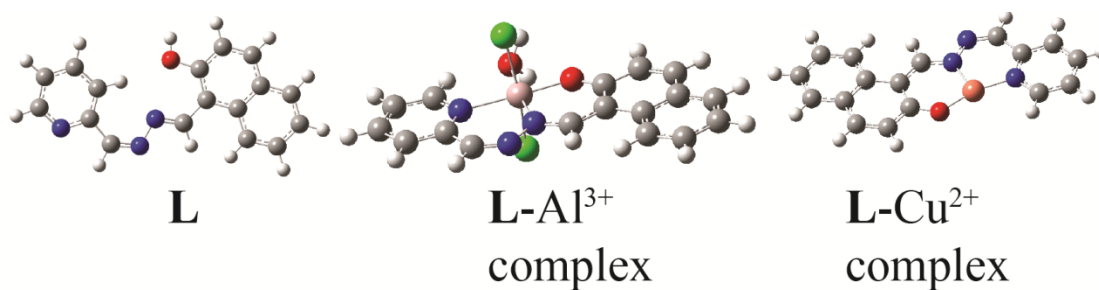


Figure S18. Optimized structures of **L**, **L-Al³⁺** complex and **L-Cu²⁺** complex. The calculations were performed using B3LYP/6-31 G (d,p) as implemented on Gaussian 03.

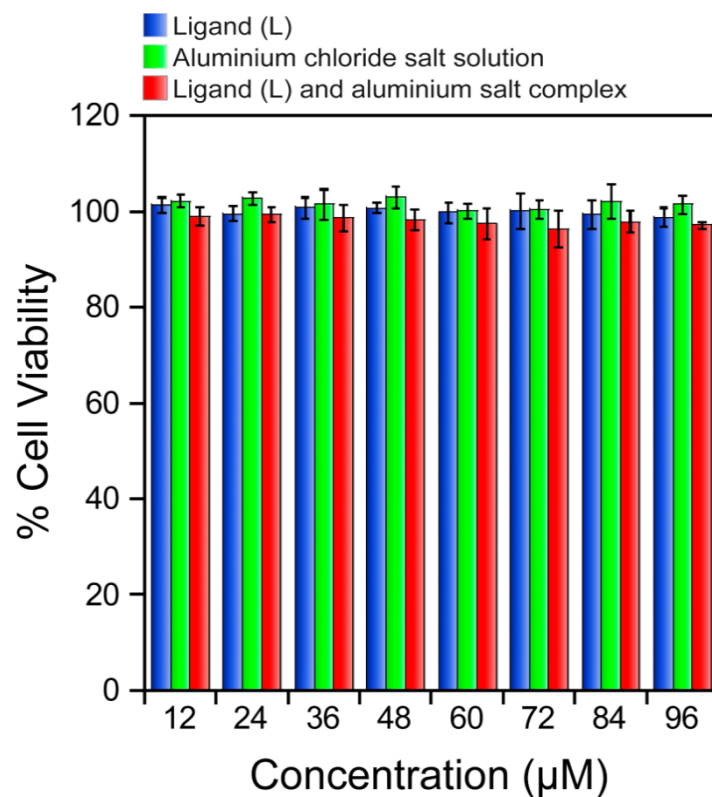


Figure S19. MTT-based assay to ascertain the cytotoxic effect of **L**, aluminium chloride salt and **L-Al³⁺** complex on HeLa cells.

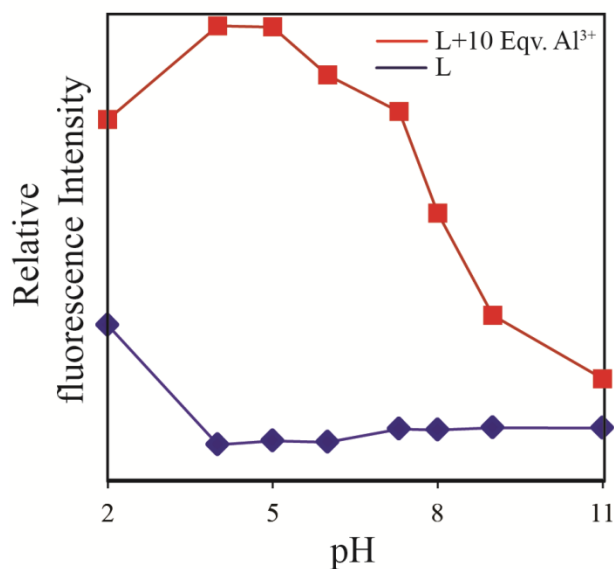


Figure S20. Dependence of the fluorescence intensity of **L** and **L-Al³⁺** on pH. Blue trace: **L** (10 μM) and red trace: **L** with excess (20.0 equivalents) of **Al³⁺**.

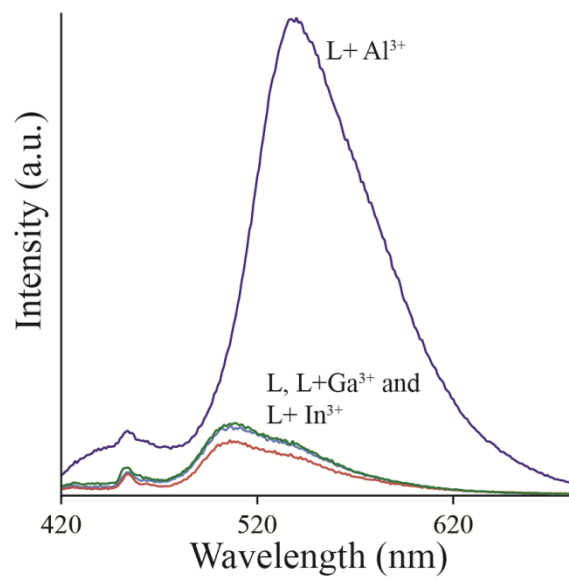


Figure S21. Fluorescence spectra of **L** (10 μ M) in presence of excess of Al³⁺, Ga³⁺ and In³⁺. λ_{ex} = 400 nm.

Table S1. Important orbitals and the energies of **L**. The calculations were performed using B3LYP/6-31 G (d,p) as implemented on Gaussian 03.

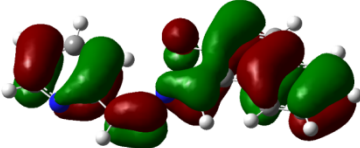
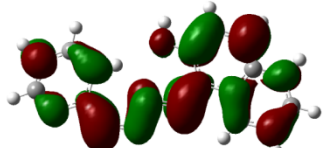
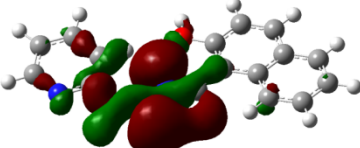
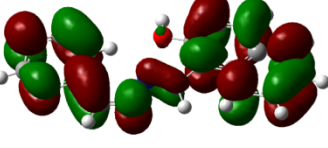
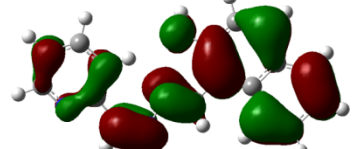
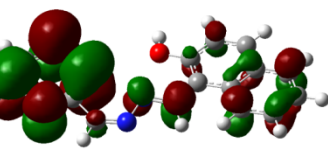
Occupied Orbitals	Energy (eV)	Vacant Orbitals	Energy (eV)
<p>HOMO-2</p> 	-6.5492	<p>LUMO</p> 	-1.9758
<p>HOMO-1</p> 	-5.8942	<p>LUMO+1</p> 	-1.0778
<p>HOMO</p> 	-5.6609	<p>LUMO+2</p> 	-0.4123

Table S2. Crystal parameters and refinement data.

Code name	L
Empirical formula	C ₁₇ H ₁₃ N ₃ O
Formula weight	275.30275.30
Cryst syst	Monoclinic
a (Å)	17.916(5)
b (Å)	4.6430(12)
c (Å)	20.248(12)
α (degree)	90.00
β (degree)	124.13(3)
γ (degree)	90.00
V (Å ³)	1394.2(10)
Space group	<i>P2₁/c</i>
Z value	4
ρ (cal)(g/cm ³)	1.312
μ (Mo K α) (mm ⁻¹)	0.085
T(K)	298(2)
R1; wR2 (I> 2 σ (I))	0.0969; 0.1463
R1; wR2(all)	0.1839 ; 0.1715
Residual electron density (e Å ⁻³)	0.284/-0.238
Good-of-fit	1.362
Reflection measured	3664
Unique reflns	2136
Reflection parameters	123
CCDC No.	1000232

References:

1. SAINT and *XPREP*, 5.1 ed.; Siemens Industrial Automation Inc.: Madison, WI, 1995. Sheldrick, G. M.
2. *SADABS, empirical absorption Correction Program*; University of Göttingen: Göttingen, Germany, 1997.
3. G. M. Sheldrick, *SHELXTL Reference Manual: Version 5.1*; Bruker AXS: Madison, WI, 1997.
4. G. M. Sheldrick, *SHELXL-97: Program for Crystal Structure Refinement*; University of Göttingen: Göttingen, Germany, 1997.
5. Mercury 2.3 Supplied with Cambridge Structural Database; CCDC: Cambridge, U.K., 2011 - 2012.
6. M. J. Frisch, G. W. Trucks, H. B. Schlegel, G. E. Scuseria, M. A. Robb, J. R. Cheeseman, J. A. Montgomery, Jr., T. Vreven, K. N. Kudin, J. C. Burant, J. M. Millam, S. S. Iyengar, J. Tomasi, V. Barone, B. Mennucci, M. Cossi, G. Scalmani, N. Rega, G. A. Petersson, H. Nakatsuji, M. Hada, M. Ehara, K. Toyota, R. Fukuda, J. Hasegawa, M. Ishida, T. Nakajima, Y. Honda, O. Kitao, H. Nakai, M. Klene, X. Li, J. E. Knox, H. P. Hratchian, J. B. Cross, V. Bakken, C. Adamo, J. Jaramillo, R. Gomperts, R. E. Stratmann, O. Yazyev, A. J. Austin, R. Cammi, C. Pomelli, J. W. Ochterski, P. Y. Ayala, K. Morokuma, G. A. Voth, P. Salvador, J. J. Dannenberg, V. G. Zakrzewski, S. Dapprich, A. D. Daniels, M. C. Strain, O. Farkas, D. K. Malick, A. D. Rabuck, K. Raghavachari, J. B. Foresman, J. V. Ortiz, Q. Cui, A. G. Baboul, S. Clifford, J. Cioslowski, B. B. Stefanov, G. Liu, A. Liashenko, P. Piskorz, I. Komaromi, R. L. Martin, D. J. Fox, T. Keith, M. A. Al-Laham, C. Y. Peng, A. Nanayakkara, M. Challacombe, P. M. W. Gill, B. Johnson, W. Chen, M. W. Wong, C. Gonzalez, and J. A. Pople, *Gaussian 03, Revision E.01*, Gaussian, Inc., Wallingford CT, 2004.